**Coupled Systems Mechanics,** *Vol. 12, No. 5 (2023) 419-428*
https://doi.org/10.12989/csm.2023.12.5.419


# Nonlinear viscous material model

Ivica Kožar*, Ivana Ban and Ivan Zambon

*Faculty of Civil Engineering, University of Rijeka, 51000, Rijeka, Croatia*

*(Received May 11, 2023, Revised July 20, 2023, Accepted July 21, 2023)*

**Abstract.** We have developed a model for estimating the parameters of viscous materials from indirect tensile tests for asphalt. This is a simple Burger nonlinear rheological two-cell model or standard model. At the same time, we begin to develop a more versatile and complex multi-cell model. The simple model is validated using experimental load-displacement results from laboratory tests: The recorded displacements are used as input values and the measured force data are simulated with the model. The optimal model parameters are estimated using the Levenberg-Marquardt method and a very good agreement between the experimental results and the model calculations is shown. However, not all parts of the model are active in the loading phase of the experiment, so we extended the validation of the model to the simulation of the relaxation behaviour. In this stage, the other model parameters are activated and the simulation results are consistent with the literature. At this stage, we have estimated the parameters only for the two-cell uniaxial model, but further work will include results for the multi-cell model.

**Keywords:** differential-algebraic equations; indirect asphalt tension test; nonlinear Burger's rheological model; parameter estimation; relaxation

## 1. Introduction

Asphalt mixtures are characterised by viscous behaviour under load, i.e., displacement increases at constant load. To optimise the behaviour of asphalt mixtures, it is useful to have a numerical material model that describes well the relationship between the load and the displacement. One could use a linear or nonlinear viscous (time-dependent) material model, usually with temperature-dependent properties, Kožar and Pranjić (2022). The simplest rheological model suitable for the analysis of asphalt mixtures is the Burger (or standard) rheological model, which consists of a Kelvin and a Maxwell rheological element connected in series, see Simo and Hughes (1998). Burger's classical model is time-dependent but linear, meaning that all four parameters (spring stiffness and dashpot viscosity for the Maxwell and Kelvin parts of the model) are constant in time. It was the preferred model for a long time because an analytical solution could be found for a constant load or displacement. Moreover, the creep (or relaxation) function could be determined analytically, see (Ornaghi *et al.* 2020). Here we introduce the nonlinear model where both springs of the model are described by an exponentially decaying force-displacement law, see Kožar *et al.* (2012). This model can only be solved numerically, but it describes the

*Corresponding author, Professor, E-mail: ivica.kozar@gradri.uniri.hr


http://www.techno-press.org/?journal=csm&subpage=8 ISSN: 2234-2184 (Print), 2234-2192 (Online)

experimental conditions much better. In addition, we have developed a general procedure for generating arbitrary complex rheological models consisting of Maxwell and/or Kelvin components. An example of this more complex multi-cell model is presented in the paper, but without quantitative validation. This more complex multi-cell model is still under development, comparable to the model in Kožar *et al.* (2018), Kožar and Rukavina (2019).

The main innovation in this paper is the mathematical description of the problem: the experimental sample is modelled as a nonlinear dynamical system. Initially, there is a similarity with lattice models (Nikolić *et al.* 2018), but unlike lattice or finite element models, there are no element or global matrices and the structure is modelled as a dynamical system, i.e., a system of nonlinear differential equations. An introduction to dynamical systems can be found in many sources, e.g., Hirsh, Smale, Devaney (2004).

The model is validated in a numerical example where it is applied to experimental data. The laboratory experiments used to test asphalt specimens are based on indirect tensile tests. In these tests, a cylindrical specimen is loaded along the edge to failure while force and displacement are recorded at the machine jaw. The load is applied very slowly because viscous materials are sensitive to the loading rate, Kožar *et al.* (2018), Kožar and Rukavina (2019). The displacement from the experiment is used as input to the model and the force response is calculated. To match the two, the model parameters need to be optimised. At the moment, we only use the simplest two-cell nonlinear Burger model, which can only describe the uniaxial behaviour of the specimen. This optimisation is performed numerically using the Levenberg-Marquardt method to minimise the optimisation function. During the optimisation, it is found that only the Maxwell part of the model minimises the objective function. The activation of the other, Kelvin part, occurs only during the relaxation phase, i.e., after the load is removed from the sample. This type of behaviour is also modelled, although there are no experimental data for this phase. Consequently, we have qualitatively compared the relaxation data with the literature and found a very good agreement.

The model parameters were numerically optimised to account for the experimental relationship between load and displacement. There is excellent agreement between the model and the experimental load-displacement curve. Further validation of our nonlinear viscous material model will be performed through additional experimental testing.

## 2. Experimental analysis

The analysis of the behaviour of asphalt mixtures of different composition with different influencing parameters related to the viscoelastic character of the material was carried out experimentally with an indirect tensile test on prepared asphalt samples. The test is standardised by HRN EN 12697-23:2003 and is performed to determine the indirect tensile strength of the tested specimen and the material properties that are important for the behaviour of the flexible pavement structure in use-permanent deformation, i.e., creep and fatigue resistance, i.e., the appearance of cracks in the material, see Zielinski (2019), (Barman *et al.* 2018). The experimental analysis was performed in two phases. In the first phase, the prepared specimens were tested to determine the influence of the composition of the mixture and the test temperature on the level of the peak force at which the failure of the specimen occurred (indirect tensile strength value as a control parameter). In the second phase, specimens that showed extreme behaviour in the first phase-the lowest and the highest indirect tensile strength-were selected and tested at different temperatures and deformation rates to determine the influence of the properties of the mixture of

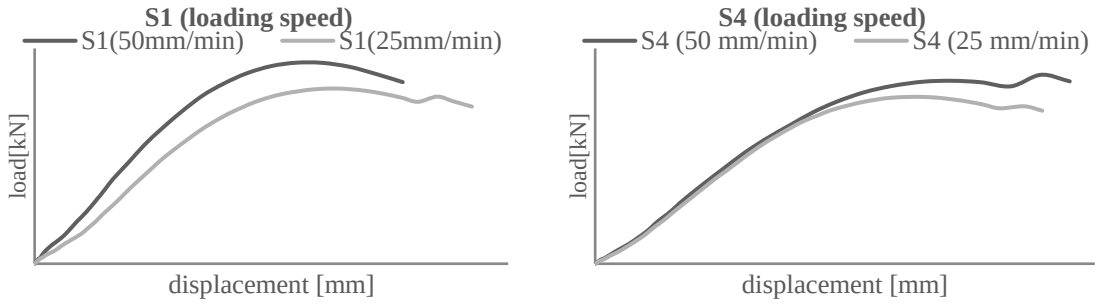


Fig. 1 Qualitative results for experimental on cylindrical asphalt specimens under different loading speeds

test conditions on the behaviour of the specimen during the indirect tensile test (diagram analysis force-displacement).

The analysis of the results of the first phase of the experiment shows that the bitumen content in the mixture significantly affects the value of the indirect tensile strength of the specimen, in such a way that a higher bitumen content in the mixture usually leads to a higher value of the indirect tensile strength. The effect of bitumen content in the mixture on the value of indirect tensile strength is greater at lower test temperatures, and generally the mixtures at lower test temperatures achieve a higher value of indirect tensile strength. Since the mixtures with the smallest and the largest bitumen content showed the most different behaviour with respect to the test temperature, they were selected to continue the experimental analysis in the second phase. All tests were carried out in the laboratory of the Faculty of Civil Engineering in Rijeka.

From Fig. 1 it can be seen that asphalt is sensitive to the rate of deformation (it also reacts to temperature, but this is not dealt with in this paper). Further description of the experimental setup, asphalt mixture design, samples preparation procedure and obtained results can be found in Kožar and Pranjić (2022).

## 3. Mathematical model

Burger's rheological model is commonly used for modeling asphalt mixtures, Mackiewicz and Szydlo (2019). This work is based on Burger's model or standard rheological model described, for example, in Simo and Hughes (1998). We have also attempted to develop and use a more elaborate but general rheological model, the multi-cell model, as in Kožar and Rukavina (2019). Burger's model can only describe uniaxial force-displacement relationships, as the results from the experiment, while the complex multi-cell model can describe complex 2D displacement fields, i.e., from experiments where multiple points are tracked in time (which is not the case in our experiment, so there are no data to test this model).

### *3.1 Burger model*

The Burger or standard model is shown in Fig. 2(a)) and the behaviour of its nonlinear springs is shown in Fig. 2(b)). It is a simple two-cell model consisting of the Maxwell and Kelvin rheological models. In our example, this model is nonlinear in its elastic parts, i.e., both springs

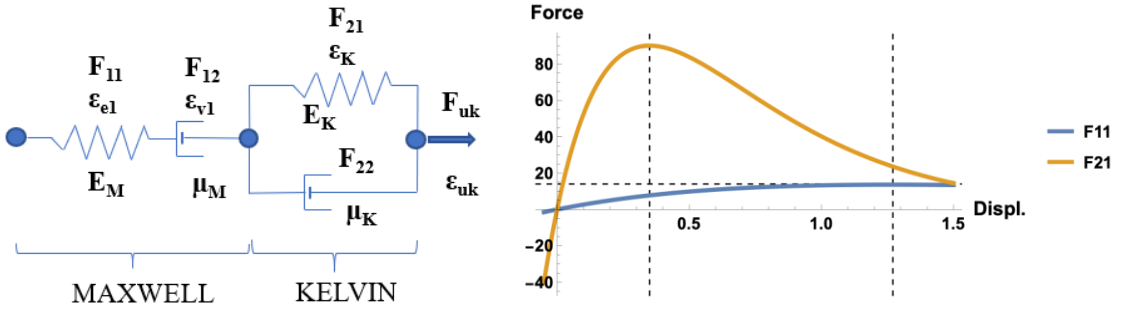


(a) (b)

Fig. 2 (a) Simple single-cell Burger's rheological model; (b) nonlinear elastic spring behaviour and their peak positions

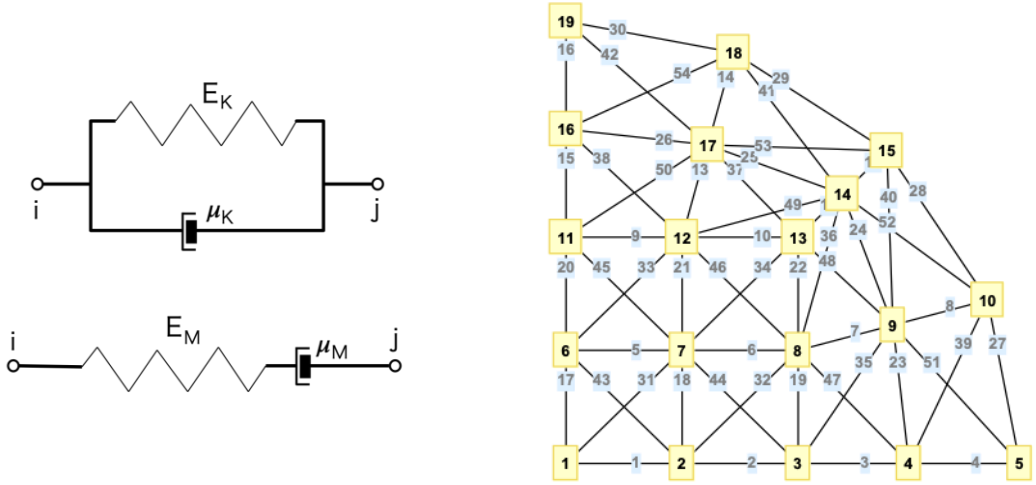


(a) (b)

Fig. 3 (a) simple single cells (Kelvin or Maxwell) forming the multicellular model; (b) more elaborate multicellular material model representing a quarter of the asphalt sample

obey exponential softening laws, as shown in Fig. 2(b)) and Eq. (1). Note that the springs behave differently in tension and in compression.

The mathematical formulation of a single-cell model is a system of differential-algebraic equations.

$$\begin{aligned} F_{11}(\varepsilon_{e1}(t)) &= \mu_M \frac{d\varepsilon_{v1}(t)}{dt} \\ F_{21}(\varepsilon_K(t)) + \mu_K \frac{d\varepsilon_K(t)}{dt} &= \mu_M \frac{d\varepsilon_{v1}(t)}{dt} \\ \varepsilon_{e1}(t) + \varepsilon_{v1}(t) + \varepsilon_K(t) &= \varepsilon_a(t) \end{aligned} \tag{1}$$

with $F_{11}(\varepsilon_{e1}) = \varepsilon_{e1} E_M \exp\left(-\frac{\varepsilon_{e1}}{a_M}\right)$ and $F_{21}(\varepsilon_K) = \varepsilon_K E_K \exp\left(-\frac{\varepsilon_K}{a_K}\right)$.

In the above equation the unknown variables are $\varepsilon_{e1}$, $\varepsilon_{v1}$ and $\varepsilon_K$, which are all functions of the pseudo-time $t$. This model has six parameters: the viscosities $\mu_M$ and $\mu_K$, the elastic moduli $E_M$ and

$E_K$, and the parameters $a_M$ and $a_K$ associated with the peaks of the elastic springs (the indices M and K represent the Maxwell and Kelvin models, respectively).

### *3.2 Multi-cell model*

In the multicellular model, each bar represents either the Maxwell or the Kelvin model, i.e., each bar corresponds to either part of the Burger model from Fig. 2(a)).

The multicellular model in Fig. 3 represents a quarter of the asphalt sample, with each node connected to a line consisting of either a nonlinear Maxwell or a nonlinear Kelvin rheology model (Fig. 3(a)). Each node can be either supported or loaded with force or displacement. In our example, the supports represent the symmetry constraints and node 19 is loaded by the prescribed displacement.

The mathematical formulation of the multi-cell model can be found in Kožar and Rukavina (2019), here without mass (purely rheological model). It is represented by a system of differential-algebraic equations, one differential equation in the *x*-direction and one in the *y*-direction for each node. In addition, the Maxwell model has an equation for the viscous force equilibrium for the internal degree of freedom.

### *3.3 Parameter optimisation*

The parameters of the model should be optimised to achieve agreement between the experimental and calculated (predicted) results. Of the six parameters, we successfully optimised the spring parameters of the Maxwell part of the model, $a_M$ and $E_M$ (the activation/exponential parameter and the modulus of the nonlinear elastic spring). The viscosity parameter $\mu_M$ has no significant effect on the results and the Kelvin part of the model is not relevant for the interpretation of the experimental data (we are only concerned with the loading of the sample). In Fig. 4 we have minimisation functions for parameters, a) for $a_M$ and $E_M$ for Maxwell part and b) for two spring moduli $E_M$ and $E_K$. It is obvious that the modulus $E_K$ does not contribute to the description of the experiment. However, as will be shown later, the Kelvin part of the model is important for the relaxation in the model, which is not analysed in the presented experiments.

The parameter estimation is formulated as an optimisation problem solved by the Levenberg-Marquardt method. The minimisation function for the optimisation problem is

$$S_{err} = \sum_{im=1}^{nm} [F\delta_{im} - Fm(\delta_{im}, a, E)]^2 \tag{3}$$

where $S_{err}$ is the cumulative error, $F\delta_{im}$ are measured values at measuring points *im* (from the experimentally determined load-displacement curve), and $Fm$ are expected values from the model, which depend on the parameters we want to determine (parameters $a_M$ and $E_M$, or any others).

Minimisation procedure leads to iterative explicit equations for each parameter calculation, e.g., for the parameter *a*

$$\Delta a = \frac{\sum_{im}[F\delta_{im} - Fm(\delta_{im}, a, E)]X_{im}}{\sum_{im}(X_{im})^2} \tag{4}$$

Here, each parameter can have either *M* or *K* index (belonging to the appropriate part of the Burger's model). Moreover, *X* is the sensitivity parameter calculated at each measuring point, i.e., $X = \frac{\partial Fm}{\partial a}$. Procedure is iterative and parameter update is additive, $a = a + \Delta a$. Other parameters are calculated in a similar manner.

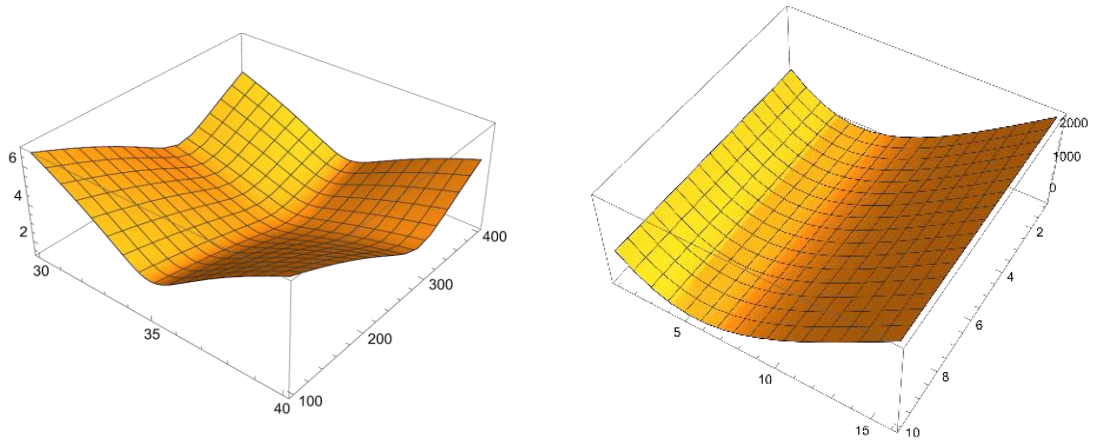


(a) (b)

Fig. 4 Minimisation functions for (a) Maxwell parameters; (b) Maxwell and Kelvin elastic moduli

As it will be seen later, the modulus $E_K$ becomes important in the relaxation phase of the loading, i.e., when the loading force disappears after the material is shrinking due to the accumulated internal energy.

## 4. Numerical example

Validation of the model in terms of (Kožar *et al.* 2022) is performed by comparison with the results of experiments conducted in two phases according to the standard HRN EN 12697-23:2003. We neglected the temperature dependence of asphalt and analysed only its viscous properties. The models used for the analysis are shown in Figs. 2 and 3. The response for the Burger model of Fig. 2 is determined for the loading and unloading (relaxation) phases; the multicellular model was evaluated only qualitatively.

The experimental force-displacement curve measured slightly after the failure of the specimen is shown in Fig. 5. The force-displacement curve obtained from Eq. (1) is also shown in Fig. 5 for comparison. The model parameters that led to the response in Fig. 5 were determined using the Levenberg-Marquardt method, as in Kožar *et al.* (2018). In addition to the Levenberg-Marquardt method, we also tried the least squares method. It gives slightly worse agreement in the last part of the load-displacement curve due to the excessive number of points at the beginning of the loading. However, improvements to the least squares method are not the subject of this article.

### *4.1 Loading phase*

In the loading phase, we specify the displacement and calculate the total force in the model. This is consistent with experimental results consisting of force and displacement measurements on the machine jaw, see Fig. 7. Note: It is possible to prescribe the force, but since there is softening in the force-displacement diagram, this loading process can only end near the upper end of the force-displacement curve. The behaviour in the loading phase is completely determined by the Maxwell part of the model, as you can see in Fig. 4(b). This is the reason for calculating the

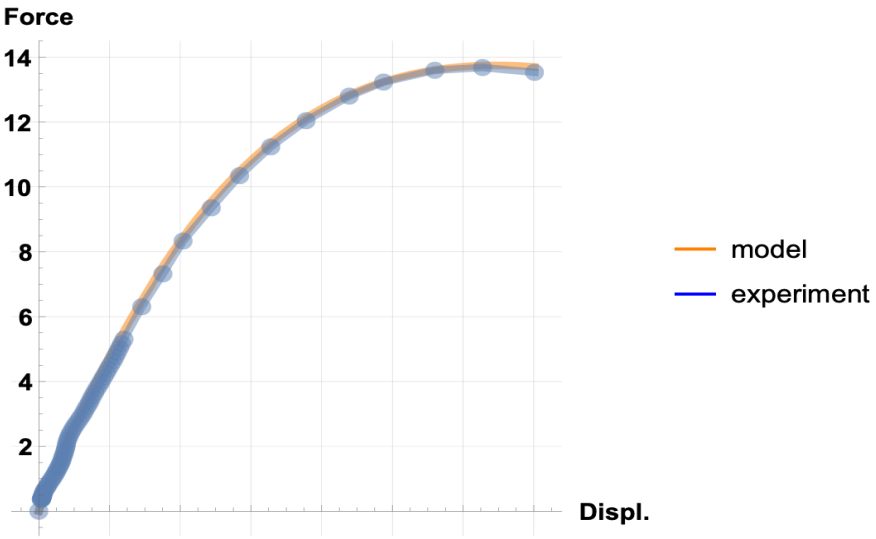


Fig. 5 Comparison of the experimental results and the model calculation

relaxation response of the model, although there is no experimental data for this part.

The behaviour of the presented model in the loading phase is shown in Fig. 5 where we see an excellent agreement between the experimental data and the model results.

### *4.2 Unloading phase*

We have attempted to test the model in the unloading/relaxation phase to determine the significance of the Kelvin parameters. For further theoretical discussion of relaxation, see, for example, (Ornaghi *et al.* 2020), Ibrahimbegovic (2009), Lemaitre and Chaboche (1994). Basically, the unloading is determined by the relaxation function of the material, which in turn is an inverse of the creep function. Here, the unloading is performed after the model is first stretched to a certain degree and then relaxed. For our nonlinear model, it is not easy to find a closed form for the relaxation function. Instead, we calculated the response of the model numerically, but even this approach is not straightforward. Namely, after the loading phase, the initial and boundary conditions change. Moreover, in the absence of the relaxation function, we need to find suitable boundary conditions so that the system of algebraic differential equations is solvable. In our case, we have assumed proportional energy release rates for the Maxwell and Kelvin parts of the model. The resulting force-displacement function for two different initial loads (corresponding to the experimental results) is shown in Fig. 6.

Unfortunately, we do not have relaxation results for our samples, so we rely on the literature for comparison. Fig. 6 corresponds to the typical relaxation values from the literature, i.e., compare e.g., with Lemaitre and Chaboche (1994).

### *4.3 Multi-cell model*

In the multicell model, Fig. 3(b), node 19 is loaded with the prescribed displacement: that from the experiment, and the reaction force is to be determined. Nodes 1 to 5 and nodes 6, 11, 16 and 19

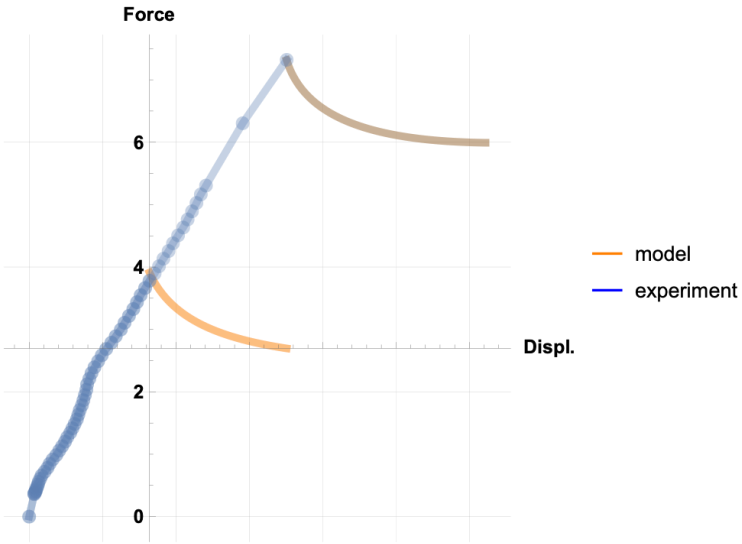


Fig. 6 Comparison of the experimental results and the relaxation calculation of the nonlinear Burger's model for two different initial loadings

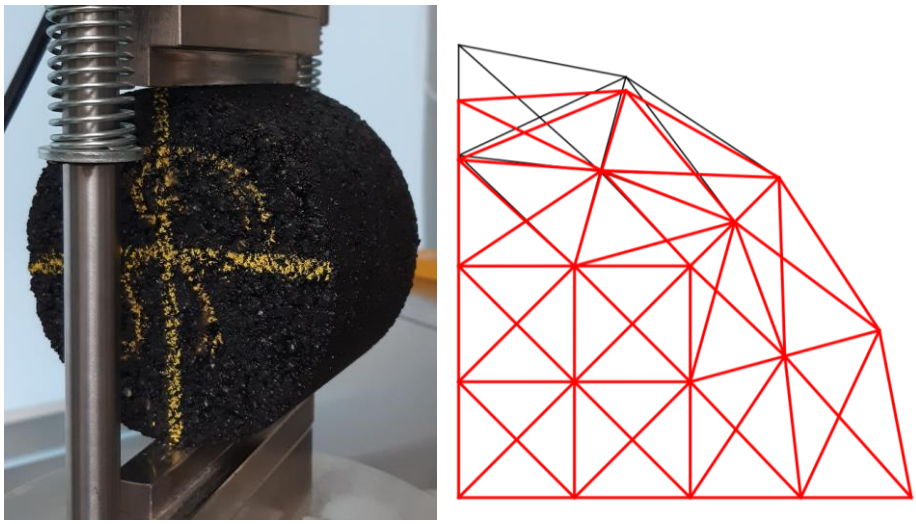

Fig. 7 Comparison of the experimental results and the model calculation

mimic the symmetry conditions. The multi-cell model consists of 38 differential equations describing the global force-displacement equilibrium and 54 differential equations describing the internal force equilibrium, for a total of 92 differential equations. All 92 differential equations are generated in the text form, one of which is shown in Eq. (2)

$$\begin{gathered}\{20.\,\epsilon v_4'(t) = 2.\,e^{10.(0.409554x_4(t)-0.409554x_5(t)+\epsilon v_4(t)+0.)} \\ \left(-0.409554x_4(t) + 0.409554x_5(t) - \epsilon v_4(t)\right), \\ \epsilon v_4(0) = 0\}\end{gathered} \tag{2}$$

The equations are automatically formulated using a proprietary program written in Wolfram Mathematica (2023); solution time is about 1 to 2 seconds. The resulting displacements can be animated. The final stage of deformation of the specimen is shown in Fig. 5 along with the experimental setup. More details on the formulation and solution of this system of differential equations can be found in Kožar *et al.* (2012), Kožar *et al.* (2018). Note: Due to the internal degrees of freedom in the Maxwell model, one has to solve many more equations than there are external degrees of freedom (displacements).

In Fig. 5 we only visually compare the experiment with the model results. A detailed comparison is not possible because we only traced one point during the test. However, we see a satisfactory agreement between the shape of the sample in the experiment and the shape of the deformed model (after calculation). We could say that the multicellular model is promising, but further investigation is needed.

## 5. Conclusions

We develop a model for estimating parameters from indirect tensile tests for asphalt. For this purpose, we have developed two models: a simple but nonlinear Burger model and a more complex nonlinear multi-cell model. At this stage, we have estimated the parameters only for the standard uniaxial Burger model, for which there is a very good agreement between the experimental results and the model calculations. In addition, we have extended our model beyond the currently available experimental tests and shown that the model is also capable of mimicking relaxation behaviour. Although the relaxation analysis requires the specification of additional initial and boundary conditions, the model can be considered suitable for describing simple (uniaxial) laboratory tests on asphalt.

In the future, we plan to extend the model to include temperature-dependent parameters. This is easy to accomplish since the temperature dependence is only loosely coupled to the existing parameters. In addition, in the future we will also develop results for the multicellular model and a suitable inverse method to estimate it’s parameters.

## Acknowledgments

This work was supported by project HRZZ 7926 “Separation of parameter influence in engineering modeling and parameter identification”, project KK.01.1.1.04.0056 “Structure integrity in energy and transportation” and University of Rijeka grant ‘uniri-tehnic-18-108’, for which we gratefully acknowledge.

## References

Barman, M., Rouzbeh Ghabchi, R., Singh, D., Zaman, M. and Commuri, S. (2018), “An alternative analysis of indirect tensile test results for evaluating fatigue characteristics of asphalt mixes”, *Constr. Build. Mater.*, **166**, 204-213. https://doi.org/10.1016/j.conbuildmat.2018.01.049.

Hirsh, M.W., Smale, S. and Devaney, R.L. (2004), *Differential Equations, Dynamical Systems and An Introduction to Chaos*, Elsevier, Amsterdam.

Ibrahimbegovic, A. (2009), *Nonlinear Solid Mechanics: Theoretical Formulations and Finite Element Solution Methods*, Vol. 160, Springer, Science & Business Media.

Kožar, I. and Pranjić I. (2022), "Nonlinear model for analysis of asphalt mixtures", *10th International Congress of Croatian Society of Mechanics*, Pula, September.

Kožar, I. and Rukavina, T. (2019), "The effect of material density on load rate sensitivity in nonlinear viscoelastic material models", *Arch. Appl. Mech*., **89**, 873-883. https://doi.org/10.1007/s00419-018-1448-9.

Kožar, I., Bede, N., Mrakovčić, S. and Božić, Ž. (2022), "Verification of a fracture model for fiber reinforced concrete beams in bending", *Eng. Fail. Anal.*, **138**, 106378. https://doi.org/10.1016/j.engfailanal.2022.106378.

Kožar, I., Ibrahimbegovic, A. and Rukavina, T. (2018), "Material model for load rate sensitivity", *Couple. Syst. Mech.*, **7**(2), 141-162. https://doi.org/10.12989/csm.2018.7.2.141.

Kožar, I., Ožbolt, J. and Pecak, T. (2012), "Load-rate sensitivity in 1D non-linear viscoelastic model", *Key Eng. Mater*., **488-489**, 731-734. https://doi.org/10.4028/www.scientific.net/KEM.488-489.731.

Kožar, I., Torić Malić, N. and Rukavina, T. (2018), "Inverse model for pullout determination of steel fibers", *Couple. Syst. Mech.*, **7**(2), 197-209. https://doi.org/10.12989/csm.2018.7.2.197.

Lemaitre, J. and Chaboche, L.J. (1994), *Mechanics of Solid Materials*, Cambridge University Press, Cambridge.

Mackiewicz, P. and Szydlo, A. (2019), "Viscoelastic parameters of asphalt mixtures identified in static and dynamic tests", *Mater.*, **12**, 2084. https://doi.org/10.3390/ma12132084.

Nikolić, M., Karavelić, E., Ibrahimbegovic, A. and Miščević, P. (2018), "Lattice element models and their peculiarities", *Arch. Comput. Meth. Eng*., **25**(3), 753-784. https://doi.org/10.1007/s11831-017-9210-y.

Ornaghi, H.L. Jr., Almeida, J.H.S. Jr., Monticeli, F.M. and Neves, R.M. (2020), "Stress relaxation, creep, and recovery of carbon fiber non-crimp fabric composites", *Compos. Part C*, **3**, 100051. https://doi.org/10.1016/j.jcomc.2020.100051.

Simo, J. and Hughes, T. (1998), *Computational Inelasticity*, Springer, New York.

Wolfram Research Inc., Mathematica (2023), https://www.wolfram.com/mathematica/

Zielinski, P. (2019), "Indirect tensile test as a simple method for rut resistance evaluation of asphalt concrete", *Arch. Civil Eng.*, **65**(3), 31-43. https://doi.org/10.2478/ace-2019-0032.